Journal of the European Ceramic Society **18** (1998) 879–890

PII: S0955-2219(97)00216-1
0955-2219/98/$19.00 + 0.00

Ultra-Micro Indentation Technique used for Examination of Mechanical Properties Close to an HIPed Surface of Silicon Nitride

A. K. Westman,[a]* M. V. Swain,[b] T. J. Bell[b] and A. Bendeli[b]

[a]Department of Materials and Manufacturing, Luleå University of Technology, S-971 87 Luleå, Sweden
[b]CSIRO, Division of Applied Physics, Lindfield, NSW 2070, Australia

(Received 14 February 1997; accepted 20 November 1997)

Abstract

Ultra-micro indentation using both pointed and spherical tipped indenters has been used to characterise mechanical properties of silicon nitride densified by glass encapsulated hot isostatic pressing (HIP). Young's modulus and hardness have been studied as a function of distance to the interface between silicon nitride and the encapsulation glass. The Young's modulus values are 10 to 20% lower in the close vicinity of the silicon nitride surface compared to bulk values. At distances of 75 to 150 microns from the glass–silicon nitride interface, bulk values are measured. The differences in hardness values between the region close to the surface and the bulk is less pronounced. A possible explanation for these gradients is formation of new phases at the surface of the silicon nitride. Routines for the calibration of both the pointed and spherical tipped indenters are presented. © *1998 Elsevier Science Limited. All rights reserved*

1 Introduction

Since structural ceramics in general have high hardness, are wear resistant and can withstand high temperatures they are not easily machined. This implies that high costs are involved in machining of structural ceramics after densification. To minimise or, even better, eliminate the need for machining of dense ceramics several issues have to be taken into consideration. One elementary demand is to be able to densify a powder body of desired component shape. When this is possible the shrinkage during densification has to be controlled. It has to be reproducible and predictable. The shape stability during processing, from green body to dense ceramic, is also essential. The glass encapsulated HIP process has a strong potential to meet these demands. Dense components of complicated shape can be produced.[1] With minimised or eliminated machining of the densified component, the quality of the surface region and the 'as-received' surface are of primary importance. The surface is often the part of the component exhibiting the highest stresses and subjected to the most severe environment. The focus of the present study is the evaluation of possible gradients in the mechanical properties as a function of distance to the 'as-HIPed' surface. The ultra-micro indentation technique was chosen for this investigation since it provides a method suitable for evaluating gradients in mechanical properties over rather short distances.

A model system of ceramic and encapsulation glass was chosen. The model system contained silicon nitride, one of the more important structural ceramics, and borosilicate glass which is known to be used as encapsulation glass for silicon nitride. To the silicon nitride has been added 3 w/o of yttrium oxide as a sintering aid. Since the encapsulating glass is in intimate contact with the surface of the ceramic component it might have an influence on the resulting surface properties. Therefore, three different compositions of the borosilicate glasses were used to determine the influence of glass properties without introducing new elements into the system. A more thorough description of the model system used is given in Ref. 2.

In the HIP process the charge is heated at ambient pressure to a temperature at which the glass is soft enough for pressure application. After pressure is applied, the heating is continued with subsequently increasing pressure until the peak

*To whom correspondence should be addressed.

temperature and pressure is reached. The present study examines the mechanical properties of samples after a complete densification cycle.

Micro indentation is a technique for evaluation of material behaviour under stress with only a limited amount of material involved in the measurements. A load is applied to the material via an indenter and the material response is recorded. With the ultra-micro indentation technique, the load can be less than 1 mN, which may result in imprints in the range of fractions of a micrometer. This means that mechanical properties such as hardness and Young's modulus can be determined for very small volumes of materials; for thin films or for different phases in a composite. When ordinary micro-indentation is used, the material response is calculated as the projected area of the remaining imprint by measuring the diagonals of the imprint using a microscope. The same technique cannot be used with ultra-micro indentation imprints due to their small sizes. Instead, the depth of the indentation is used to determine the size of the imprint. Penetration is continuously measured and registered during the experiment as a function of load applied. There are several commercially available instruments for this type of measurement. In this work the UMIS-2000 has been used and Ref. 3 gives a detailed description of the apparatus.

During the last decade there has been continual progress and discussions on how to interpret the data from the load-displacement test results and translate them into conventional mechanical properties. Basic theories have been presented and equations established for calculating e.g. hardness and Young's modulus, see e.g. Refs 4–7. Despite this progress more fundamental information such as the stress–strain behaviour of the material during deformation with pointed indenters is not fully understood, especially for hard materials such as ceramics. The spherical shaped indenter with its axi-symmetric contact results in a simpler elastic-plastic deformation pattern including an initial elastic response prior to yielding that is more easily described. With all these methods of indentation, some correction factors such as indenter tip calibration are involved in the actual analysis, because of the non-perfect form of the indenters. At present, the ultra-micro indentation techniques are often used for comparison between similar materials and less as an absolute measurement of a materials behaviour. Here the results with a pointed Berkovich indenter have been compared with those of a spherically tipped indenter, which may be considered as a reference. Moreover, in Appendix C, 'Notes on corrections', A and B are discussed, equations and corrections used for the calculations.

2 Experimental

The hot isostatic pressing densification parameters for the samples in this study were 1750°C, 160 MPa with a hold time of 1 h. Densified samples are examined both with and without glass encapsulation remaining on the outside of the specimen. Bulk samples, not exposed to the encapsulation glass, were examined for comparison.

In Table 1 is shown the combinations of the different samples and corresponding encapsulation glasses. The boron oxide/silicon dioxide ratio differs between the different glasses and some glass characterisation is also shown in the table. After densification sample (1) still contained 10% porosity and the two other samples, (2) and (3), had densities greater than 99% of the theoretical density.

The densification parameters used give microstructures typically built up of mainly equiaxed grains in the size of 0·2–0·6 microns with some more elongated grains.

The samples were prepared in the following way for indentation tests. Specimens were cut and moulded in bakelite before grinding and polishing. For the grinding steps silicon carbide papers were used down to 1600 mesh. The polishing steps consisted of long duration on a steel and subsequently tin lap, with diamond grit of three microns size. This gave a sample with a flat surface and limited curvature at the edges. The specimens were given a short final polish of approximately 15 s on paper with a one micron diamond grit slurry. Indenters of two different geometries were used in the present tests. One indenter was the commonly used Berkovich indenter, with a triangular cross-section and a face angle of 65·3°. The other had a spherical shaped tip, with a nominal radius of 10 microns. The results from the two indenters were compared in order to establish the universality of the information of the region of interest, i e close to the glass–silicon nitride interface.

As there is not yet general agreement on how to interpret the force–displacement data achieved, a brief description of the equations and assumptions used for the calculations in this work is given in the appendices. The indentations with the Berkovich indenter were performed with a maximum load of

Table 1. Encapsulation glass composition and viscosity for different samples

Sample	*Ceramic material*	*Encapsulation glass* B_2O_3/SiO_2	*Viscosity, 1450°C*
(I)	Si_3N_4(3Y[a])	30%/70%	$> 10^{4.5}$ dPas
(II)	Si_3N_4(3Y[a])	50%/50%	n.d.
(III)	Si_3N_4(3Y[a])	60%/40%	$10^{2.8}$ dPas

[a]3 w/o Y_2O_3.
n.d. means not determined.

300 mN and a contact force of 0·3 mN. The number of load increments were 30 and the same for unloading. Figure 1 shows typical force/penetration curves from these tests. The hardness and Young's modulus were calculated according to Appendix A. The indentations with the spherical indenter were performed with a somewhat different loading pattern. The tests were built up of loading/unloading steps where each unloading step was 50% of the previous load. Typical force/penetration curves for these tests are shown in Fig. 2. The maximum load was 500 mN and the contact force 0·5 mN. The hardness and Young's modulus calculations are given in Appendix B.

A discussion on the corrections for initial penetration, tip discrepancy from perfect sharpness or sphericity and compliance of the measuring system, beneath the depth-sensing device is given in Appendix C, 'Notes on corrections'.

3 Results of Measurements

The Berkovich indenter was used for measuring the silicon nitride specimens densified with different

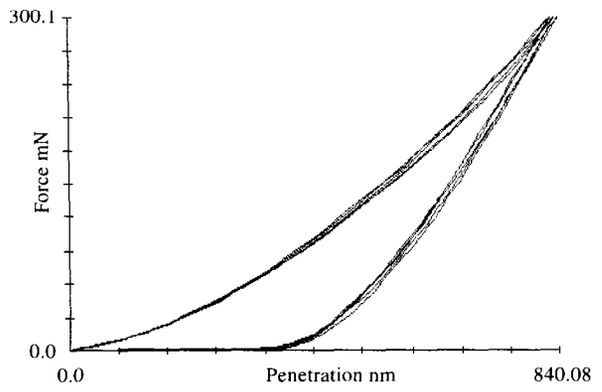

Fig. 1. Load–penetration plot, Berkovich indenter. Five different penetrations in the same plot, each built up of 30 load increments for both loading and unloading.

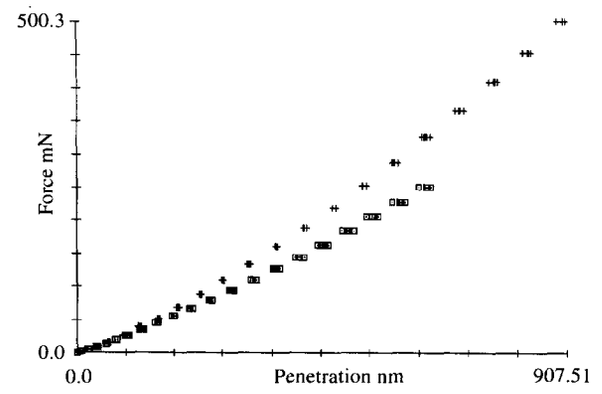

Fig. 2. Load–penetration plot, spherical indenter. Five different penetrations in the same plot. Each penetration built up of loading/unloading steps with the unloading step 50% of the previous load.

encapsulation glasses. The Young's modulus, as a function of distance from the interface between the encapsulation glass and silicon nitride, is shown in Fig. 3. Five to ten indents were made at each distance. The standard deviation is shown as bars and is mostly within the dot size. Two different measurement series on material (II) are included in the figure to show that some discrepancy was obtained between different series. However, the trends for the different materials are the same. Gradients are present with a decrease of 10–20% in Young's modulus close to the interface compared to the bulk values. The values approach the bulk data at a distance of 75 to 150 microns from the interface. It is obvious that the porous material (I) shows much lower absolute values compared to the materials densified with the other glasses. These values also show a somewhat flatter appearance close to the edge compared to the other materials but the decrease compared to the bulk is the same. Although the imprints are only a few microns wide, a sample was prepared to examine if the determined gradients were only edge phenomena, caused by the lower stiffness of the supporting material present at the edge. Bulk samples, cut after densification, were indented close to the cut edge. The results are shown in Fig. 4. A slight gradient might be present below 75 microns, but not in the same range as the material with its interface towards the encapsulation glass, Fig. 3.

Hardness as a function of distance to the interface is shown in Fig. 5. Here only very limited tendencies can be detected. The porous material (I) shows some variations in hardness where the values are somewhat lower close to the edge. Also the dense material (II) shows the same appearance but material (III) seems to have similar values in the bulk and close to the interface. For the reference bulk material, Fig. 6, no gradients in the hardness values as a function of distance to the sample edge are shown. Here one of the series showed a rather large standard deviation.

These results can be compared to those achieved with the spherical indenter. Figure 7 shows the Young's modulus values achieved with a 10 micron radius sphere. Material (I) is represented by two different series with complimentary values. Every dot represents a mean value of five indents except series I(a) with just one value for each dot. Again there is a gradient in the Young's modulus with bulk values reached at 75–150 microns from the interface. Material (I) shows a less pronounced plateau in the values than the Berkovich measurements. In Fig. 8 the corresponding hardness values are shown. The results correspond well with the ones achieved using the Berkovich indenter.

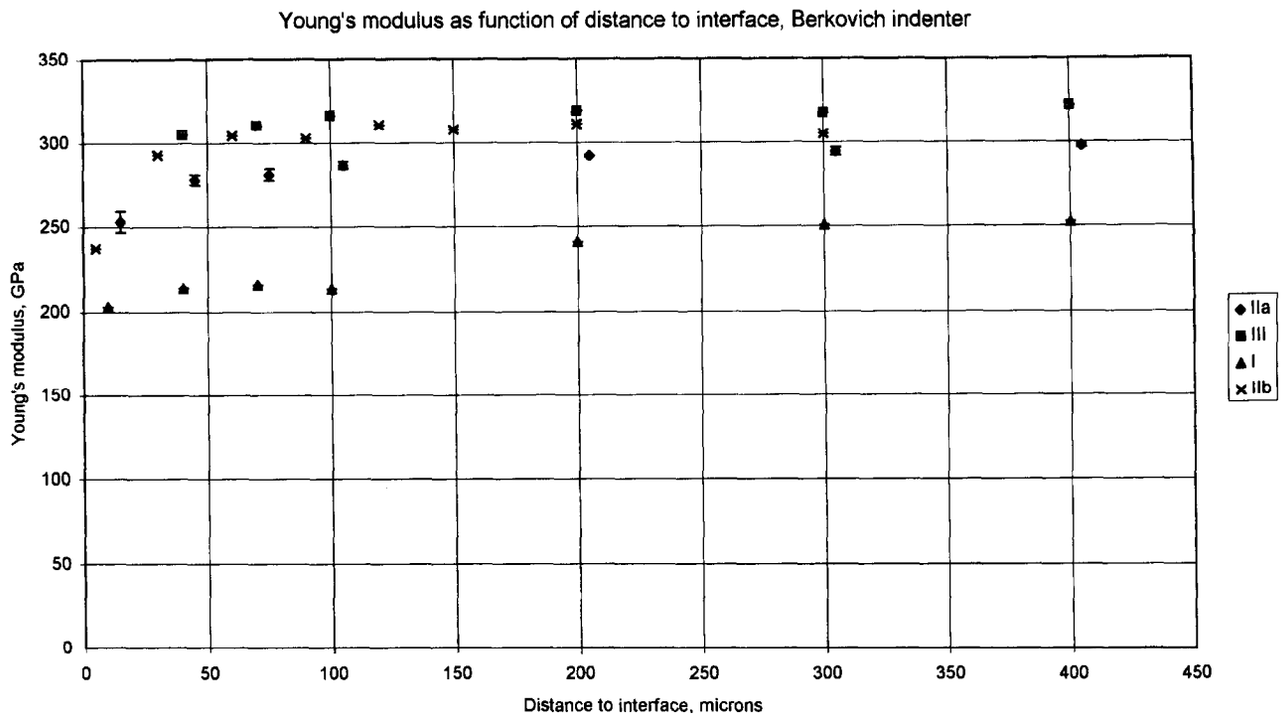

Fig. 3. Young's modulus in silicon nitride as a function of distance to the interface towards the encapsulation glass, Berkovich indenter. For specimen details, see Table 1.

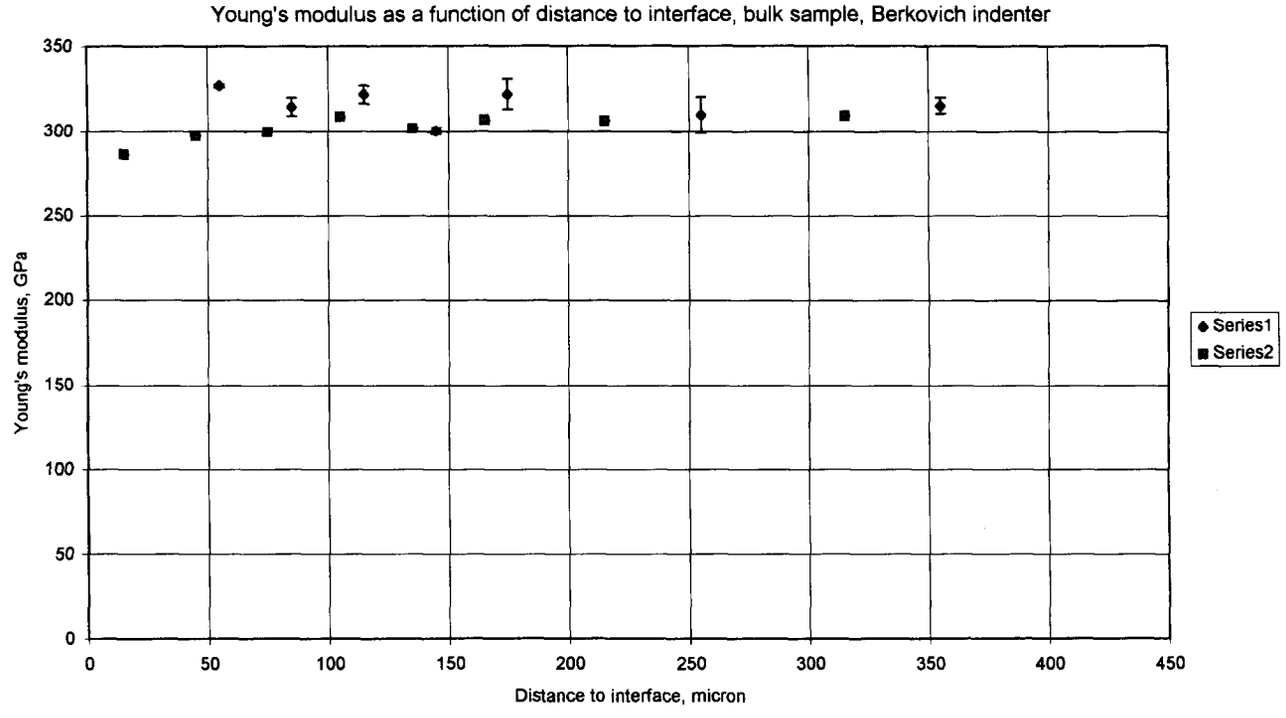

Fig. 4. Young's modulus in bulk silicon nitride as a function of distance to a cut surface, two different measurements, Berkovich indenter.

4 Discussion

In these tests with a very limited indentation depth, the influence of sample preparation must be taken into consideration. Although there may indeed be some microcracks associated with the polishing, the depth of the plastic zone and size of the impression is far greater than the depth of penetration. With the indenter size of 10 microns and an indentation of about 1 micron the contact diameter will be several microns. This will result in the volume of material under the indenter being quite large compared to the approximately 1 micron affected by surface polishing. In addition the hardness values measured at various locations indicated no influence of indenter load or depth

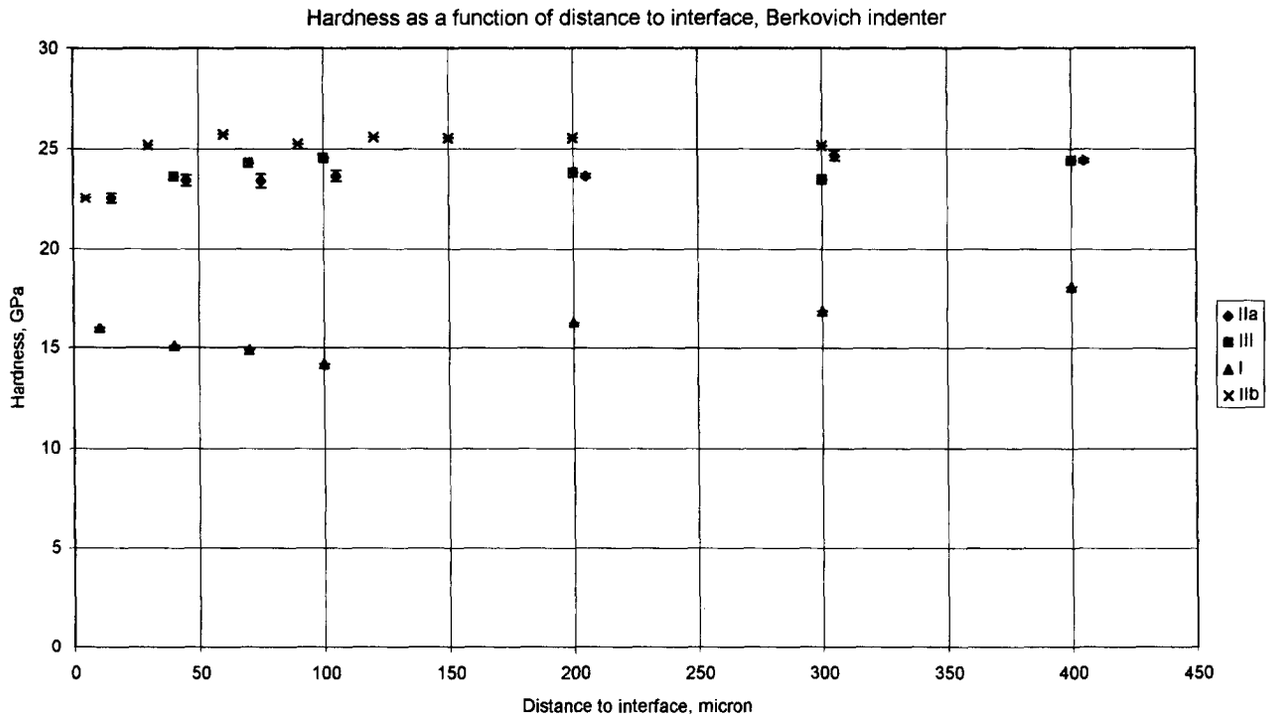

Fig. 5. Hardness in silicon nitride as a function of distance to the interface towards the encapsulation glass, Berkovich indenter. For specimen details, see Table 1.

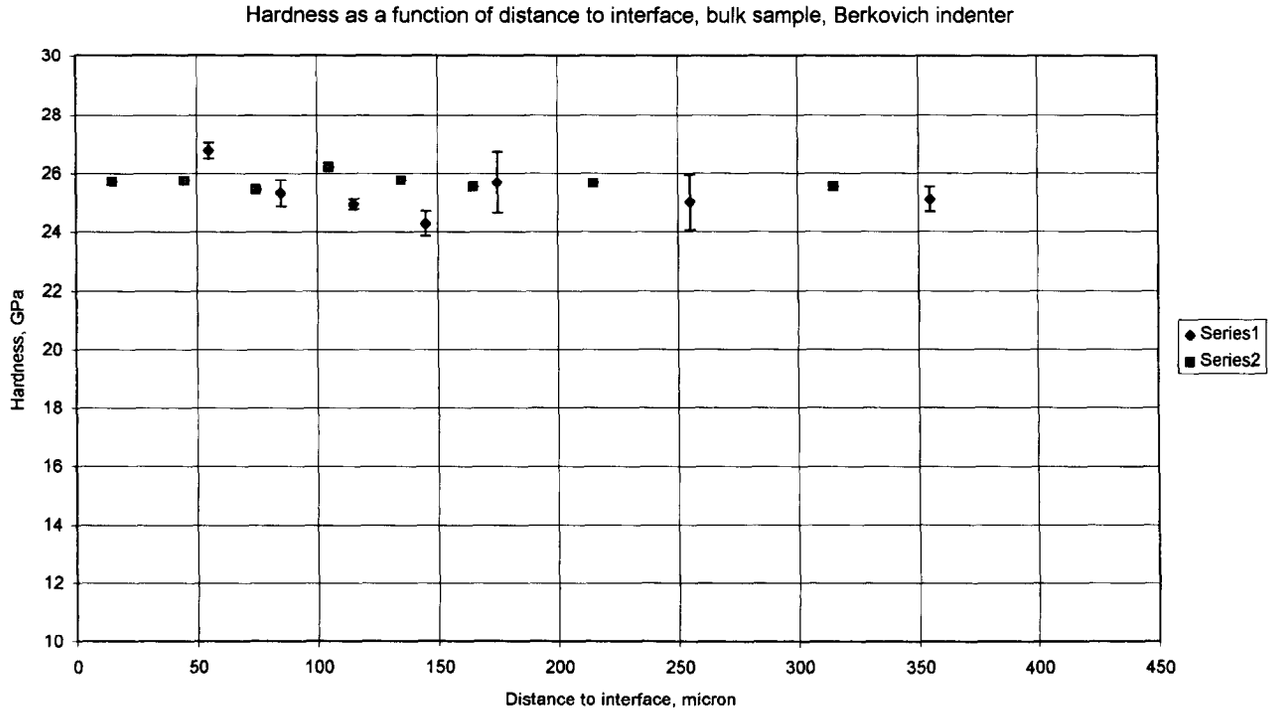

Fig. 6. Hardness in bulk silicon nitride as a function of distance to a cut surface, two different measurements, Berkovich indenter.

of penetration, hence it is considered that the effect of any minor dislocations/microcracks present is not significant. Also the fairly good agreement between the Berkovich and spherical indent results, although there are different strain situations under these indenters, indicate that the effect of surface preparation on the results could be negligible.

Both the measurements with the Berkovich and the spherical indenter have revealed gradients in Young's modulus to a distance of 75–150 microns into the bulk. The influence of the edge giving less support has been illustrated by the cut bulk sample. A small gradient was detected but not in the same range as the glass/silicon nitride surface samples. The imprints are only approximately 1 micron

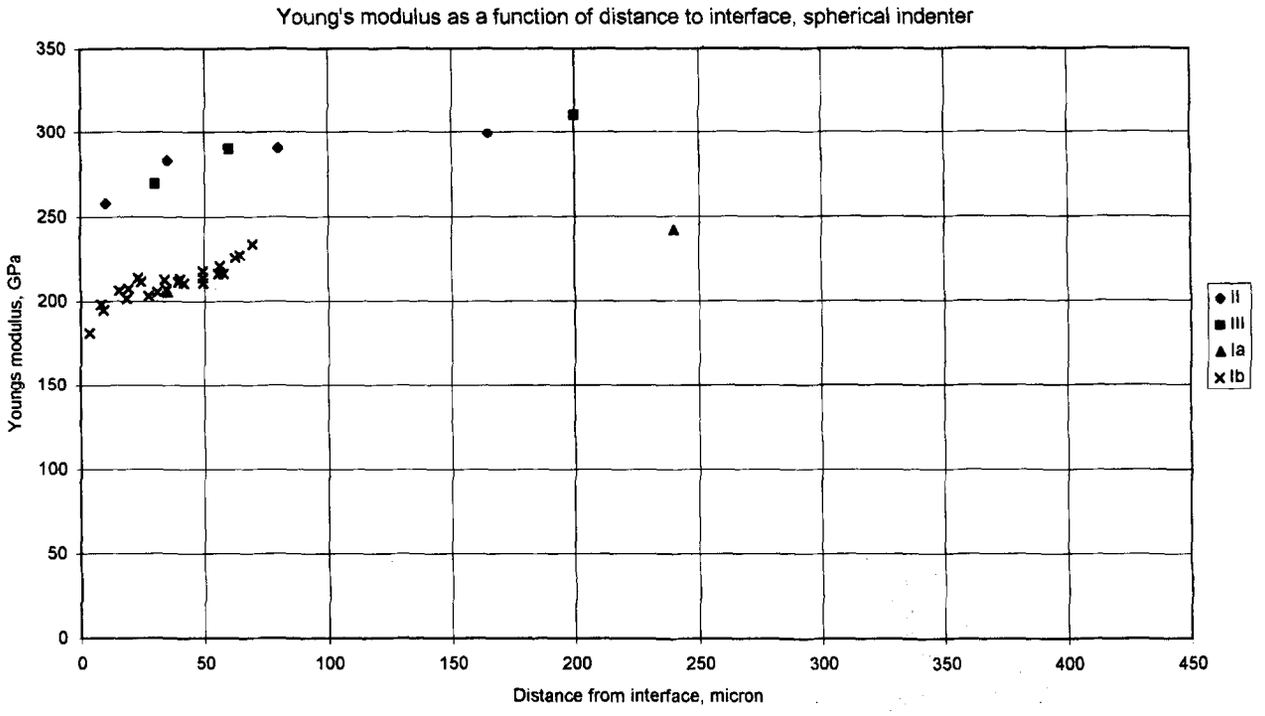

Fig. 7. Young's modulus in silicon nitride as a function of distance to the interface towards the encapsulation glass, spherical indenter. For specimen details, see Table 1.

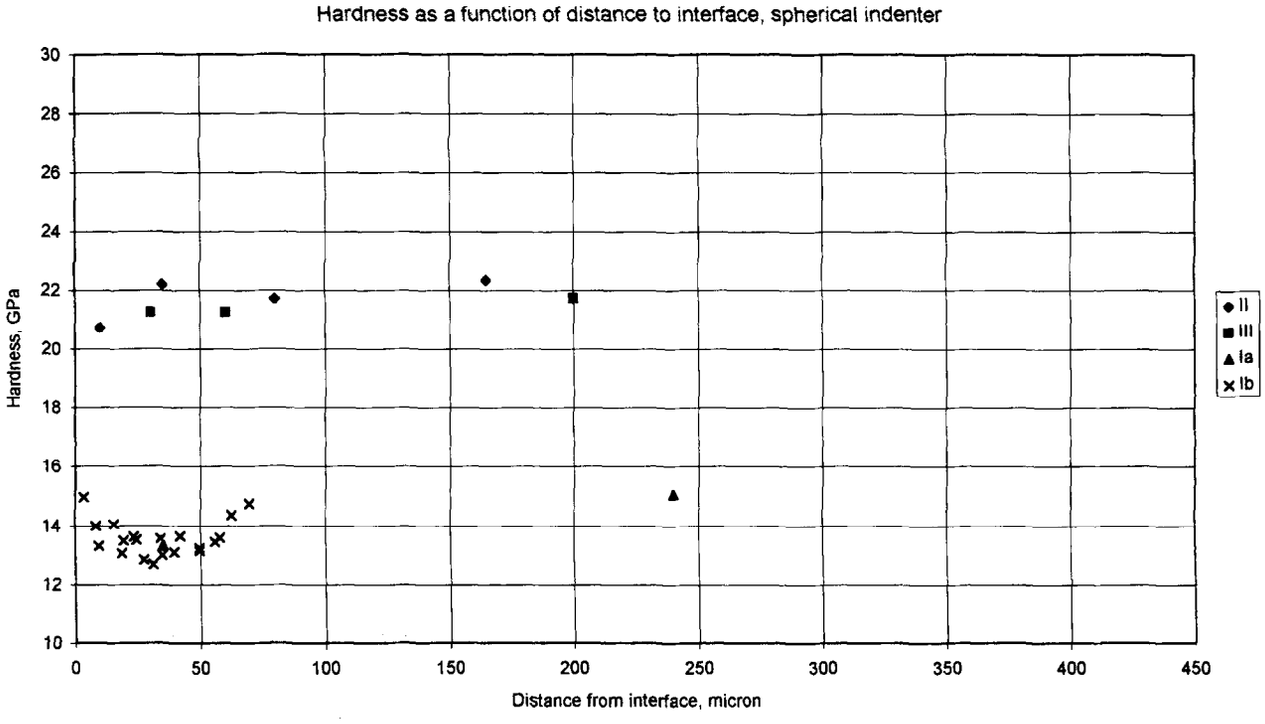

Fig. 8. Hardness in silicon nitride as a function of distance to the interface towards the encapsulation glass, spherical indenter. For specimen details, see Table 1.

in depth and 4–5 micron in width and it is unlikely they should be influenced by the edge 50–100 microns away.

One reason for the gradients might be an infiltration of the encapsulation glass into the ceramic specimen. No differences in the gradients were found for the tested different glasses. Earlier studies[8] with WDS in SEM have shown an increased amount of boron at the HIPed surface down to a depth of 20 to 150 microns into the bulk, with the same results for samples with the different encapsulation glasses. Assuming glass infiltration, the surface region could be regarded as a composite.

The Young's modulus for a mixture of different phases can be calculated according to Voigt, assuming the strain in each constituent is the same

or by Reuss, assuming the stress in each phase is the same. These two models give lower and upper bounds for the elastic moduli.[9] If the reduction in Young's modulus was caused by the lower Young's modulus of the glass (70 MPa), the amount of glass needed for a 20% reduction in modulus is calculated to be between 7% and 26%. However, in SEM studies it has not been possible to detect any significant differences between the microstructure in the surface region and the bulk and no evidence for a large amount of glass has been found. Still, due to the similar element composition of the encapsulation glass and the silicon nitride material and because of the predominance of light elements, the SEM studies cannot be considered as definitive.

Another possible reason for the lower values could be cracking. Irrespective of their origin, cracks give lower values in the mechanical properties. If there is glass in the ceramic structure, a difference in thermal expansion coefficient between the glass and the ceramic could cause stresses during cooling and hence crack formation. But these differences are quite small (in the range of some units 10^{-6} K^{-1}) and hence not creating stresses large enough for crack formation. Depending on the technique for elimination of the encapsulation glass from the ceramic surface, different degrees of mechanical damage might be created in the surface region. However, in these tests the encapsulation glass has not been removed from the silicon nitride surface. The influence of porosity on the modulus values is demonstrated in the test results for the porous sample I. A porosity of 10% is enough for a 20% reduction in modulus[9] which was found for the bulk value of sample I. However, SEM-studies of the dense samples have not given any evidence of increased porosity in this range close to the interface. A more plausible explanation for the

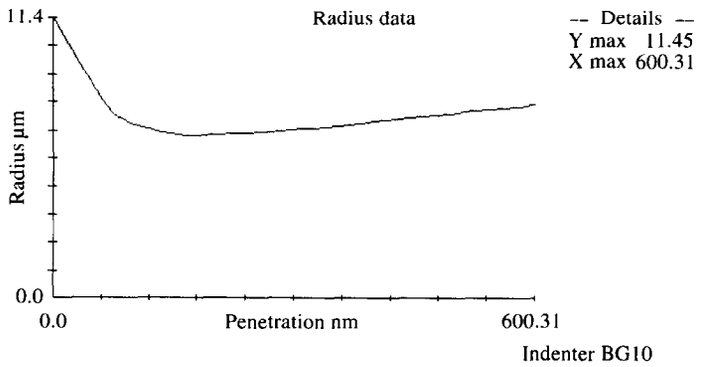

Fig. 9. Estimated tip radius as a function of penetration (spherical indenter).

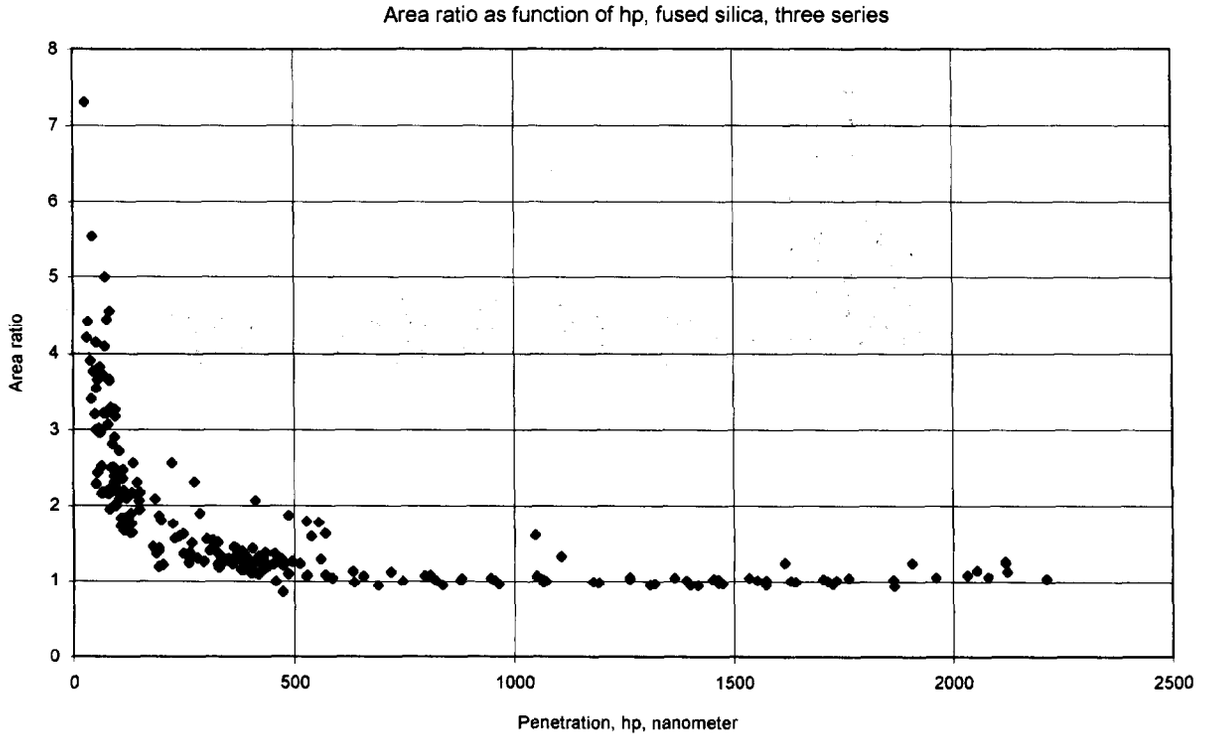

Fig. 10. Area ratio (actual contact area/theoretical contact area) as a function of contact depth (Berkovich indenter).

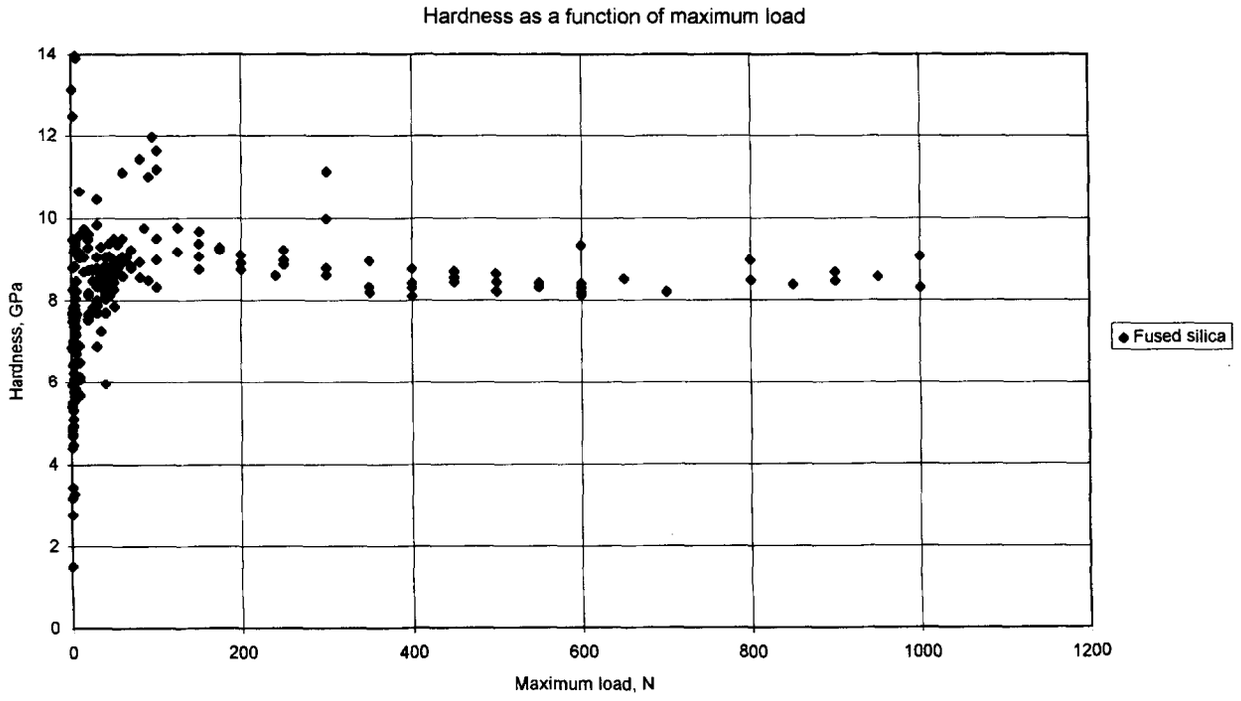

Fig. 11. Hardness as a function of maximum force in fused silica as estimated with the equation derived from the relation in Fig. 10 (Berkovich indenter).

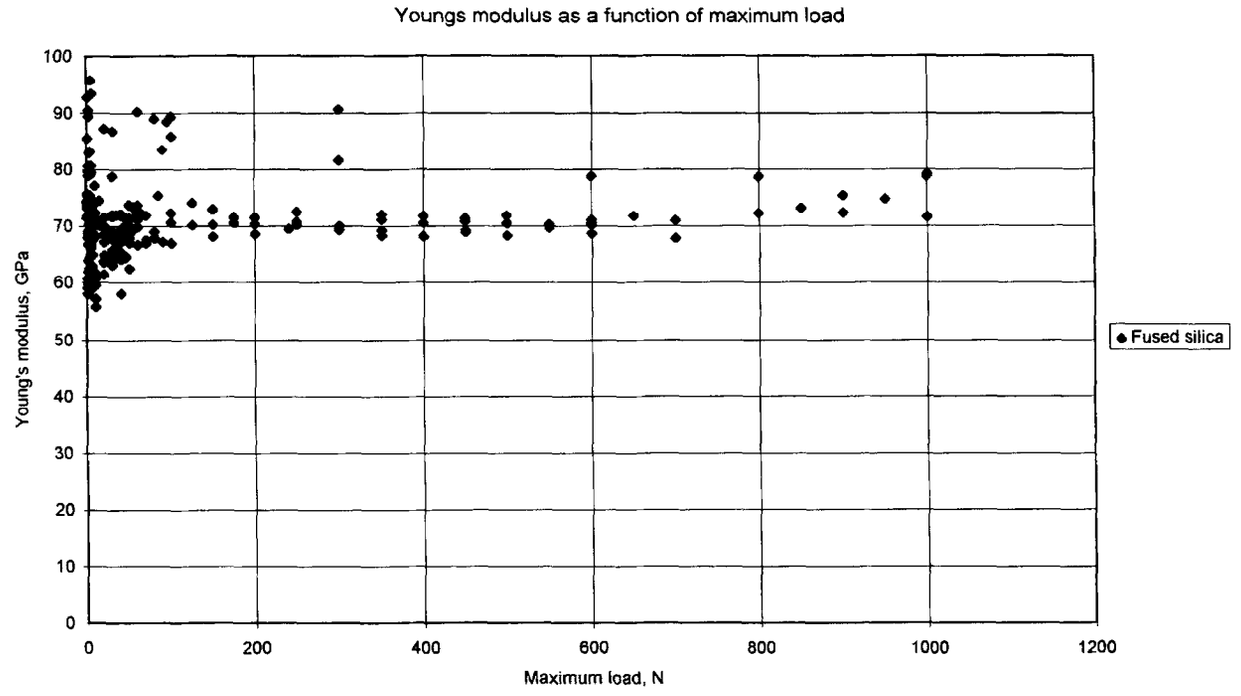

Fig. 12. Young's modulus as a function of maximum force in fused silica estimated with the equation derived from the relation in Fig. 10 (Berkovich indenter).

gradients in mechanical properties is the formation of new phases at the interface.

Westman *et al.*[10] have found that silicon oxynitride and boron nitride are thermodynamically stable in a mixture of silicon nitride in contact with borosilicate glass at conditions of silicon nitride densification. They also show that these phases are actually formed in a sample mixture of glass and silicon nitride at the peak temperature in a HIP cycle. Moreover, the silicon nitride samples in the present tests were analysed by X-ray diffraction on the surfaces after glass elimination (soft bead blasting). Silicon oxynitride was easily detected and a rough estimation of the amounts was 30–50 v/o. It was not possible to detect any boron nitride peak. However as the main peak is overlapped by a silicon nitride peak, the presence of BN cannot be excluded. A material similar to sample III has been

ground in small steps to a depth of 500 microns from the surface with XRD-measurement at each step.[2] This study showed a silicon oxynitride gradient to a depth of 150–200 microns. In the literature there are different values reported for Young's modulus of silicon oxynitride. Larker[11] gives a value of 288 GPa for a material of 91% silicon oxynitride and 9% silicon nitride. Work with oxide additives reports lower values. Billy *et al.*[12] obtained a value of 220 GPa for silicon oxynitride with 5 w/o yttrium oxide. With the value of 220 GPa, the upper and lower boundaries for a mixture of 50% silicon oxynitride and 50% silicon nitride is 257 and 265 GPa. Thus, this silicon oxynitride formation in the surface region can explain the gradients in mechanical properties. Boron nitride has a very low Young's modulus, 35 GPa, and will consequently influence in the same direction. The hardness of silicon oxynitride densified by HIP is reported by Larker.[11] He found for materials containing above 85% silicon oxynitride (the rest was α- and β-silicon nitride) values comparable with the hardness of HIPed silicon nitride with 2·5 w/o Y_2O_3. Boron nitride formation will decrease the hardness.

For the correction of the imperfectly shaped Berkovich indenter tip an area relation was used, see Appendix C, 'Notes on corrections'. A_{known} (from known values of Young's modulus for a reference material) and $A_{theoretical}$ (perfect tip geometry) was plotted against the contact depth. This gives improved data analysis especially for measurement of small penetration depth.

5 Conclusions

Mechanical properties in silicon nitride as a function of distance to the interface towards the encapsulation borosilicate glass have been studied. The gradients calculated from the indents made by the Berkovich and the spherical indenter are in good agreement. Young's modulus shows a reduction of 10–20% close to the interface and bulk values at a distance of 75–150 microns. Gradients in hardness values are less pronounced.

The measured gradient in Young's modulus cannot be explained by the edge giving less support since a bulk sample, cut and measured close to the edge, only showed a minor edge effect. A plausible explanation for the gradients is formation of new phases. The amount of Si_2N_2O found at the surface of the silicon nitride specimen is enough to decrease the value of Young's modulus in the range found. Also detected depth of the Si_2N_2O gradient in similar samples corresponds well with the depth of the gradient in Young's modulus.

References

1. Larker, H. T., *Hot Isostatic Pressing, Engineered Materials Handbook*, Vol. 4, ed. S. J. Schneider *et al.* ASM International, 1991, pp. 194-201.
2. Westman, A. K. and Larker, H. T., Study on encapsulation glass/silicon nitride ceramic interaction during HIPing. In press.
3. Bell, T. J., Bendeli, A., Field, J. S., Swain, M. V. and Thwaite, E. G., The determination of surface plastic and elastic properties by ultra micro-indentation. *Meterologia*, 1991, **28**, 463–469.
4. Doerner, M. F. and Nix, W. D., A method for interpreting the data from depth-sensing indentation instruments. *J. Mater. Res*, 1986, **1**(4), 601–609.
5. Oliver, W. C. and Pharr, G. M., An improved technique for determining hardness and elastic modulus using load and displacement sensing indention experiments. *J. Mater. Res*, 1992, **7**(6), 1564–1583.
6. Fields, J. S. and Swain, M. V., A simple predictive model for spherical indentation. *J. Mater. Res*, 1993, **8**(2), 297–305.
7. Mencík, J. and Swain, M. V., Micro-indentation tests with pointed indenters. *Materials Forum*, 1994, **18**, 277–288.
8. Westman, A. K. and Larker, H. T., The interface of glass and silicon nitride in HIPing. Presented at the 97th Annual Meeting of the American Ceramic Socicty, Cincinnati, OH, April 30-May 3, 1995.
9. Kingery, W. D., Bowen, H. K. and Wilmann, D. R., *Introductions to Ceramics*, 2nd edn. John Wiley & Sons, New York, 1975.
10. Westman, A. K., Forsberg, S. and Larker, H. T., Chemical reactions in the system Si_3N_4–SiO_2–B_2O_3. *J. Eur. Ceram. Soc.*, in press.
11. Larker, R., Reaction sintering and properties of silicon oxynitride densified by hot isostatic pressing. *J. Am. Ceram. Soc.*, 1992, **75**(1), 62–66.
12. Billy, M., Boch, P., Dumazeau, C., Glandus, J. C. and Goursat, P., Preparation and properties of new silicon oxynitride based ceramics. *Ceram. Int.*, 1981, **7**(1), 13–18.
13. King, R. B., *Int. J. Solids Structures*, 1987, **23**, 1657–1664.
14. Mencík, J. and Swain, M. V., Errors associated with depth-sensing micro indentation tests. *J. Mater. Res.*, 1995, **10**(6), 1491–1501.
15. Jämting, Å., Ring, M., Ruppi, S. and Swain, M. V., Mechanical characterisation of kappa and alpha alumina films on hard metals using indentation methods. *J. Hard Mater.*, 1995, **6**, 67–87.

APPENDIX A

Calculation Berkovich indenter

Properties measured with the Berkovich indenter were calculated in the following way:

The hardness was calculated using

$$H = P/A \tag{A1}$$

where H is the hardness, P is the indenter load and A the projected area of the contact surface given by

$$A = K \times h_c^2 \tag{A2}$$

where K is a constant dependent on the indenter geometry, 24·56 for Berkovich, and h_c is the contact depth (see Fig. A1).

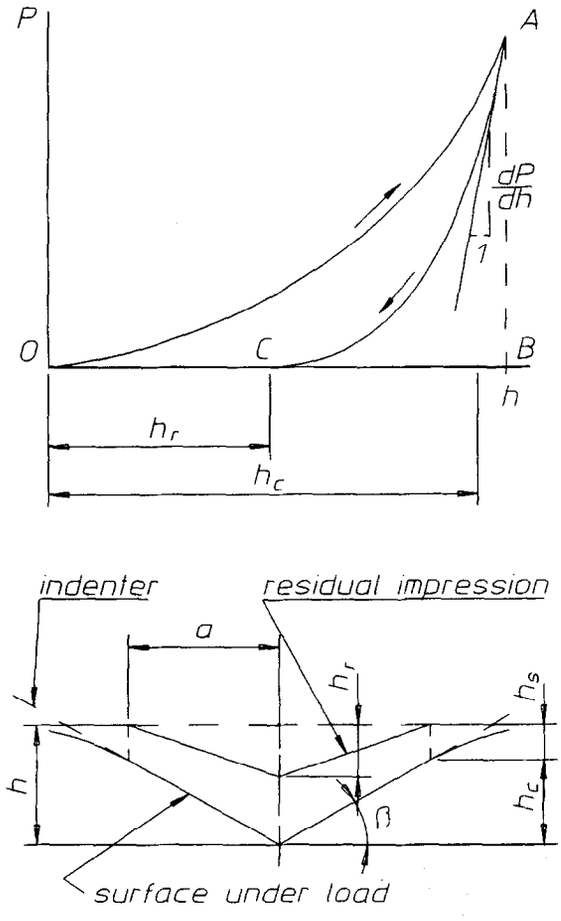

Fig. A1. Force–displacement curve and cross-section of the impression at maximum load and upon unloading (Berkovich indenter).[15]

The depth h_c is defined as

$$h_c = h - 0{\cdot}75(P^{max}/(dP/dh)) \qquad \text{(A3)}$$

the parameters being defined in Fig. A1.

The Young's modulus was calculated according to the relationship

$$E^* = k \times dP/dh \times 1/\sqrt{A} \qquad \text{(A4)}$$

k is a constant, the value $1{\cdot}034 \times 2/\sqrt{\pi}$ being used for the Berkovich indenter (see King),[13] dP/dh is the slope of the load–displacement curve at the beginning of unloading (see Fig. A1), E^* is the composite modulus (specimen + indenter) and the following relation being used to calculate the modulus of the specimen:

$$1/E^* = (1 - v_s^2)/E_s + (1 - v_i^2)/E_i \qquad \text{(A5)}$$

where s and i refer to specimen and indenter, respectively.

For a more detailed analysis underlying these relations for hardness and Young's modulus, see Mencík and Swain.[14]

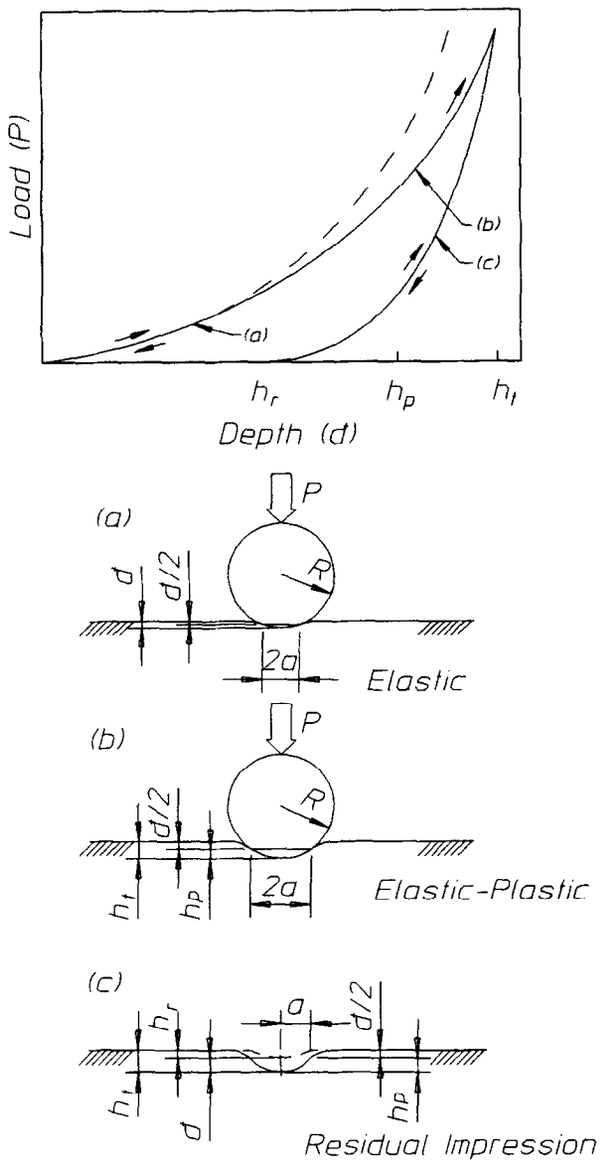

Fig. B1. Force–displacement curve and cross-section of the impression at maximum load and upon unloading (spherical indenter).[15]

APPENDIX B

Calculation spherical indenter

Data from the spherical indenter were analysed in the following way:

The hardness was calculated as Meyer's hardness, HM, i.e. mean pressure over the circle of contact:

$$HM = P/\pi a^2 \qquad \text{(B6)}$$

where P is the indenter load and a is the radius of the contact circle.

The relation between a and the penetration is given by

$$a = (2Rh_c - h_c^2)^{1/2} \qquad \text{(B7)}$$

R is the radius of the indenter tip and h_c is the contact depth component of the penetration, given

by

$$h_c = (h_t + h_r)/2 \qquad \text{(B8)}$$

where h_t is total penetration and h_r is the residual impression depth (see Fig. B1).

The Young's modulus is given by the expression

$$E^* = 3/4 \times P/(a \times \delta) \qquad \text{(B9)}$$

developed from the Hertz equation for elastic contact of a sphere on a plane or into a spherical cavity.

δ is the elastic depth recovery h_t-h_r (see Fig. B1).

Reference 6 provides a thorough discussion of the relations given above.

APPENDIX C

Notes on corrections

The expressions used for the pointed Berkovich and spherical tipped indenters assume a perfect indenter shape. However, it is impossible to achieve a perfectly sharp indenter tip and the anisotropy of a diamond single crystal prevents the achievement of perfect sphericity. Hence, there is a need for procedures to correct for these imperfections. In the present work fused silica is utilised as a reference material to establish the tip calibration. It is an isotropic amorphous material with known elastic modulus and Poison's ratio.

For the spherical indenter a reference measurement with fused silica was used to create a look up table for correction factors as a function of different depth. The known Young's modulus of silica is used to calculate the radius of the indenter. The Hertz relationship for elastic contact of a sphere into an elastic half space is:

$$\delta = (9/16)^{1/3}(P/E^*)^{2/3}(1/R)^{1/3} \qquad \text{(C1)}$$

where δ is total depth of elastic penetration, (see Fig. B1)P is the load and E^* is the composite Young's modulus [see eqn (A5), Appendix A]. With known δ, P and E^* the indenter tip radius can be estimated. When this is calculated for different loads, for different contact depths, h_p (see Fig. B1), a tip radius versus contact depth plot is obtained. Figure 9 shows an example of the estimated or effective tip radius versus contact depth for a spherical indenter with a nominal radius of 10 microns. The raw data is analysed using this changing value of radius in the calculations of hardness and Young's modulus. This analysis procedure is automatically performed using the UMIS software.

There are a number of methods whereby corrections for the tip imperfections in the Berkovich indenter may be performed. One of the procedures adds to the measured depth a small depth equivalent to material 'missing' at the tip due to bluntness. The routine is based on the theoretical square root force versus depth relation, $\sqrt{P} \sim h$, valid for an ideally sharp indenter assuming the hardness of the reference material is a constant (derived from eqns (A1) and (A2) in Appendix A). A known material is tested, load P and total measured penetration h is plotted in a diagram and an equation:

$$\sqrt{P} = kh + h_o \qquad \text{(C2)}$$

is fitted to the data points. From this expression h_o is a measure of the additional depth which should be added to the measured depth. The corrections are relatively large for smaller depths when compared to total penetrations. This method was found to give less satisfactory corrections, probably due to the assumption of constant hardness.

Another method was presented by Oliver and Pharr[5] where the contact area A is determined from the measured compliance dh/dP of a material with known Young's modulus (see eqn (A4), Appendix A). Values obtained for A (for different loads) are plotted against various contact depth, h_c, and a polynomial $A(h_c)$ is fitted to the curve. In the present work the same approach is taken but an area ratio compared with a perfectly formed indenter instead of the contact area is plotted as a function of contact depth. The indenter of interest was used to create indents with a range of different maximum loads on the fused silica reference material. The load-penetration relations were established and the depths h_c were determined. Equation (3) gives the theoretical (for a perfect indenter geometry) areas, $A_{theoretic}$, for different depth:

$$A = K \times h_c^2 \qquad \text{(C3)}$$

where K is 24·56 for a Berkovich geometry. Another area, A_{known}, was calculated by using the known value of Young's modulus for the reference silica. The area ratio $A_{known}/A_{theoretic}$ was plotted against contact depth, h_c (see Fig. 10). A power law relation was fitted to the data points below 800 nanometers. The equation for the line is:

$$y = 18{\cdot}933\, x^{-0{\cdot}4455} \qquad \text{(C4)}$$

Penetrations deeper than 800 nanometers result in a ratio of~1. The area to be used in the equation for hardness and Young's modulus calculations, eqns (A1) and (A4), Appendix A, is determined with depth h_c and the area ratio equation.

Figures 11 and 12 show the resulting hardness and Young's modulus for fused silica calculated according to this procedure. This correction technique gives improved data analysis especially for measurement of small penetration depth compared to the technique with only contact area–contact depth plot.

Another factor which has to be taken into consideration for depth corrections is the initial penetration at the near zero contact force (the minimum force the instrument can measure). The load–depth curve has to be extrapolated back to zero load to determine the point of zero penetration. This is done by using an optimised regression analysis of a simple power law fit of a chosen number of the initial data points and then extrapolating it to zero load. There is a choice in the software to select the number of points the line fit should take into account. Eight data points have typically been used in the initial penetration calculations for this work.

The third correction of the raw data takes into account the compliance of the measuring system. For the measurements with the spherical indenter a value of $0{\cdot}15\,\mathrm{nm\,mN^{-1}}$ was found to be suitable. The compliance correction for the Berkovich indentation was experimentally determined. This was done according to a method presented by Doerner and Nix.[4] A plot of dh/dP against $1/h_c$ will, according to the theory, give a straight line and the intercept at the y-axes is the compliance. Experimental data in this work with the fused silica samples did not give a perfect straight line. With increasing h_c values, lower intercept values were achieved. Reasons for this could be roughness or lack of flatness of the surfaces involved or intermediate layers with more or less stiffness. In the calculations for the fused silica the intercept was determined by using the highest h_c values (lowest $1/h_c$) since the compliance is probably measured with greater reliability at higher loads. This routine results in a compliance correction of $0{\cdot}2\,\mathrm{nm\,mN^{-1}}$ with the Berkovich indenter on fused silica. This correction also resulted in reasonable values for the parameters calculated.

In the Berkovich tests on the silicon nitride samples, which had a somewhat rougher surface finish, only a limited number of different loads were used and no accurate determination of the intercept could be achieved. In this instance a machine compliance value of $0{\cdot}00\,\mathrm{nm\,mN^{-1}}$ was chosen. The calculations gave Young's modulus values for the dense bulk material in relatively good agreement with known values for dense silicon nitride. Even if a more thorough determination of the system compliance had been made, the trends or relative values of Young's modulus or hardness would not have changed since the same maximum load and indenter tip were used in all tests.